A NOVEL COATING METHOD USED TO ENABLE MULTILAYER STRUCTURES WITH MICROSCALE SELECTIVE LASER SINTERING

A. Liao*, D. Behera*, M. A. Cullinan*

*Walker Department of Mechanical Engineering, The University of Texas at Austin, Austin, TX 78712

Abstract

The microscale selective laser sintering process (µSLS) is an additive manufacturing technique that enables the creation of metal features with sub-5 µm in-plane resolution. In this process, a layer of metal nanoparticle ink is deposited onto a substrate and positioned beneath an optical subsystem with a nanopositioning stage. Using a digital micromirror device, a laser is spatially modulated to selectively heat up particles in desired regions to cause sintering. The substrate is then moved to a coating station where a new layer of nanoparticle ink is applied atop the sintered features. Initially, the slot-die coating process was adopted as the recoating method for this technique. However, due to challenges with depositing consistent ink thickness across the recoated part and limitations with the minimum layer thickness achievable, a new approach inspired by blade coating has been developed to achieve layer thicknesses of less than 1 µm.

Introduction

The aim of developing the microscale selective laser sintering process is to manufacture three-dimensional components with sub-5 µm features, all while achieving a throughput of 60 mm^3/hr [1]. To create a single layer of a part the machine must heat a particle bed at a designated location, apply a new layer of nanoparticles onto the sintered part, and accurately position the components between successively added layers. To carry out these tasks, the current version of the machine comprises three primary subsystems: an optical sintering system, global and nanopositioning systems, and a nanoparticle ink dispensing system as shown below. These processes are iteratively executed to eventually build up a three-dimensional part.
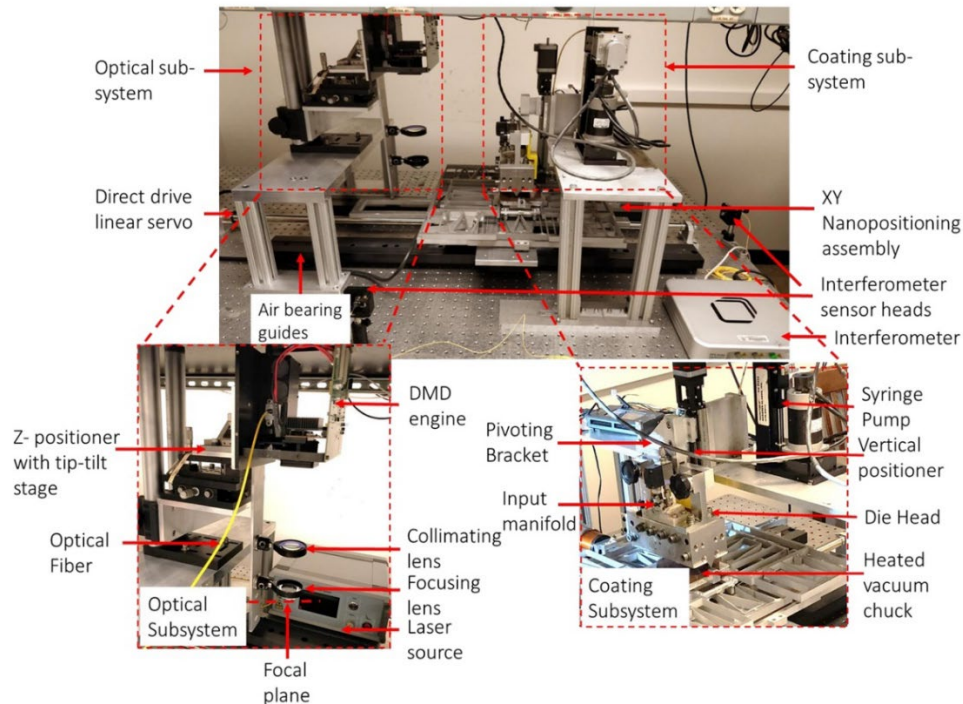

Figure 1: Diagram showing the three subsystems of the microscale selective laser sintering machine and their components [1].

Background

Because microscale selective laser sintering (µ-SLS) of metals adheres to similar principles as its larger-scale counterpart, achieving uniform deposition of nanoparticles onto previously sintered layers is crucial. Instead of utilizing micron-scale particles as seen in traditional metal powder bed fusion (PBF), µ-SLS employs metal nanoparticles to enhance process resolution. However, obtaining repeatable, densely packed layers with nanoparticles presents challenges due to their elevated surface energy and susceptibility to excessive oxidation [2]. Previous sintered structures created with nanopowders had high porosity, subpar physical attributes, and low electrical conductivity [3]. This prompted investigation into using nanoparticle inks, which consist of copper nanoparticles dispersed in an organic solvent. Initially, the slot die coating process was chosen for this process, however the films deposited by this process were too thick, and this work investigated using a different meniscus guided coating process.

Blade coating was of particular interest due to ease of setup and significantly reduced volume of ink in the meniscus. Under fluid flow condition with low capillary number ($Ca \ll 1$), Landau Levich coating theory can be used to predict the thickness of films deposited by meniscus guided processes. Capillary number is defined as the ratio between viscous drag forces and surface tension forces and can be expressed as in Equation 1 where η is the viscosity of the fluid, v is the velocity of the fluid meniscus, and γ is the surface energy of the fluid.

$$Ca = \frac{\eta v}{\gamma} \tag{1}$$

The solution derived by Le Berre et al. [2] for a is provided below in Equation 2.

$$t_{wet} = 1.34L(Ca)^{2/3} \tag{2}$$

$$L = \frac{H}{\cos\theta_1 + \cos\theta_2 - \frac{H^2}{2\kappa^{-2}}} \tag{3}$$

The geometry of the meniscus in the flow coating process is shown in the figure below, labeling where the constants in Equation 3 are from.
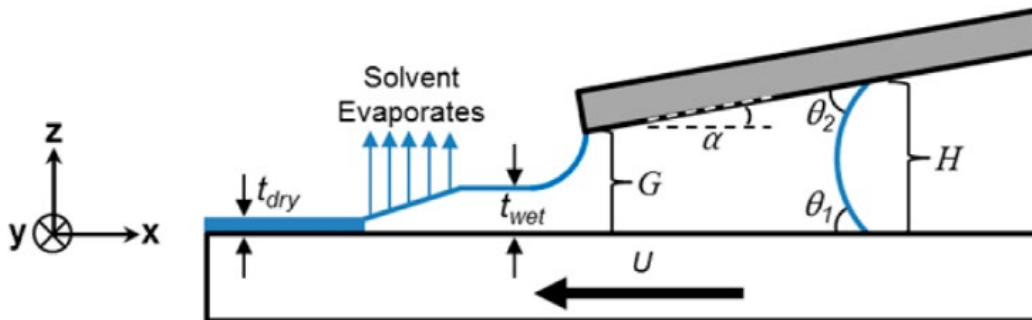

Figure 2: Diagram of the meniscus geometry in the flowcoating process [3]

This solution for wet film thicknesses deposited by the flowcoating process will be compared against the experimental results by obtaining meniscus geometry parameters.

Blade Coating Apparatus Design

The coating apparatus should be able to apply extremely thin layers of metal nanoparticle ink (less than 1 μm in thickness) onto sintered metal surfaces from the preceding layers. The coating process window, thickness, and uniformity for the previously used slot die coating procedure, are influenced by various process parameters. Given that this approach is still influenced by the meniscus, we aim to have similar control over process parameters as those employed in slot die coating. The coating device should have the ability to control the coating gap, coating speed, and volume of deposited ink. The tool that was developed was able to automate the blade positioning, ink dosage, and substrate translation steps required to deposit a thin film with the fluid entrained by the meniscus.
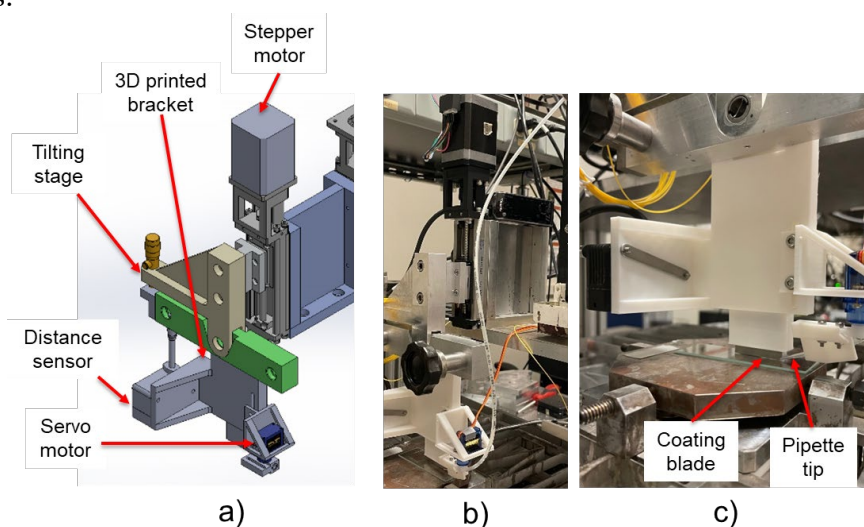

Figure 3: a) CAD model of the assembled coating device. b) Physical embodiment of the coating device. c) Zoomed in view of the custom designed 3D printed parts that hold blade, distance sensor and pipette tip.

The coating blade height was controlled using a 5-phase stepper motor (Oriental Motor) to drive a screw driven linear stage (Newport). The minimum step of the motor and the pitch of the screw results in a resolution of 1 μm, allowing for precise positioning of the blade relative to the substrate. This distance is measured using a laser triangulation distance sensor (Keyence), and an open loop stepping algorithm is used to position the blade at various heights.

Ink is delivered to the meniscus by using a syringe pump (Kloehn/IMI Norgren) with a 5 mL zero dead volume tip syringe. It is plunged by a brushless DC motor with a resolution of 24000 pulses per revolution, and lead screw with 1mm pitch, allowing us to achieve a volumetric resolution of approximately 300 nL.

To provide the substrate translation, the nanopositioning stage was used. The stage is translated along the axis aligned with the coating direction using a voice coil and a 1:1 current amplifier. To keep track of its position, an Attocube FPS 3010 interferometer is employed, featuring a Thorlabs silver mirror target attached to a 3D-printed bracket. The displacement of the stage in this axis is controlled by a PID controller with the output current of the voice coil actuator. With custom trajectory generation, we can precisely control the speed of the substrate for the coating operation.

These are all automated within LabVIEW and a schematic showing the process and the order of the steps is shown below.
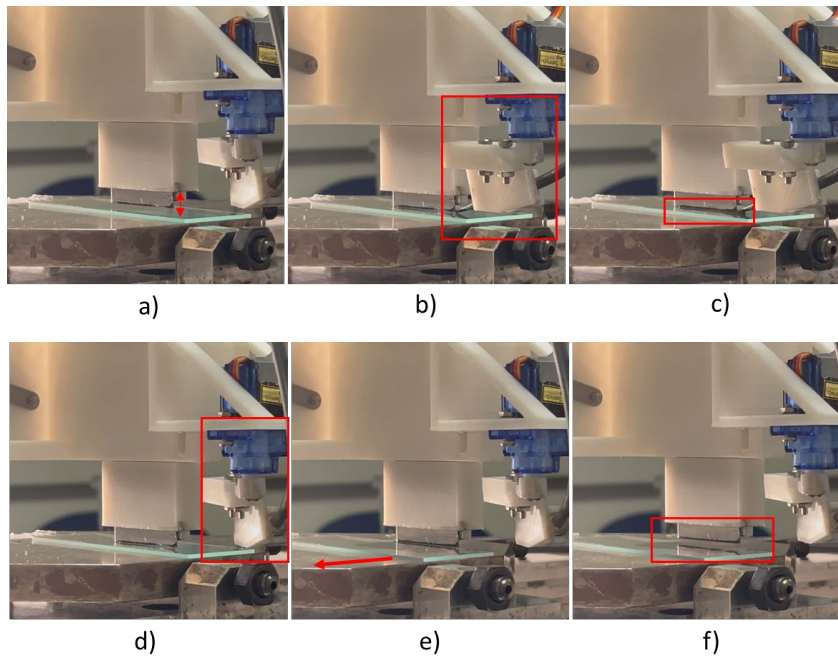
Figure 4: Sequence of the coating steps automated by the prototype coating tool. **a)** Begins with blade lifted off substrate surface pipette tip away from gap. **b)** Servo actuates pipette tip to substrate gap. **c)** Syringe pump forces ink through tubing that exits at the pipette tip, forming meniscus. **d)** Servo actuates pipette tip off glass substrate. **e)** Substrate travels with ink entrained in meniscus. **f)** Blade lifts away from substrate and breaks meniscus.

<u>Characterization of Single Layer Coating</u>

To control the thickness of the ink deposited, we want to determine relationship between coating speed and wet film thickness. The coating gap (100 μm), and volume of ink (3 μL) in the meniscus were held constant and the coating speed in these experiments ranged between 0.5 – 3 mm/s. To compare against the coating theory, images of the blade, substrate, and meniscus were taken to obtain the geometric constants used in Equation 3. Figure 5 shows the side view of the meniscus geometry and the relevant lengths and angles required to estimate the wet film thickness using Landau Levich coating theory.
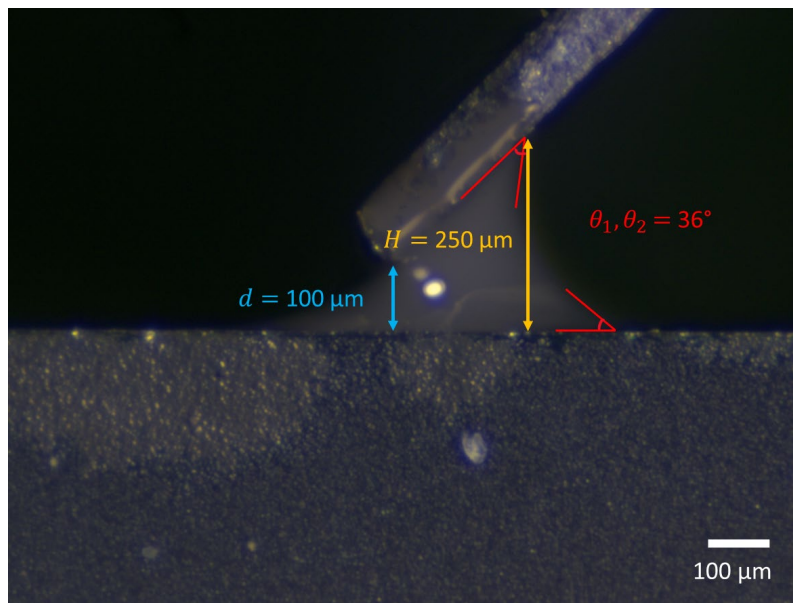

Figure 5: Image of the meniscus used to derive geometric parameters used in the calculation of predicted wet film thicknesses.

Given that the capillary number exhibits a direct proportionality to velocity (as per Equation 1), and thickness follows a power-law relationship with the capillary number (as per Equation 2), the velocity should also exhibit a power-law relationship with the thickness of the ink.
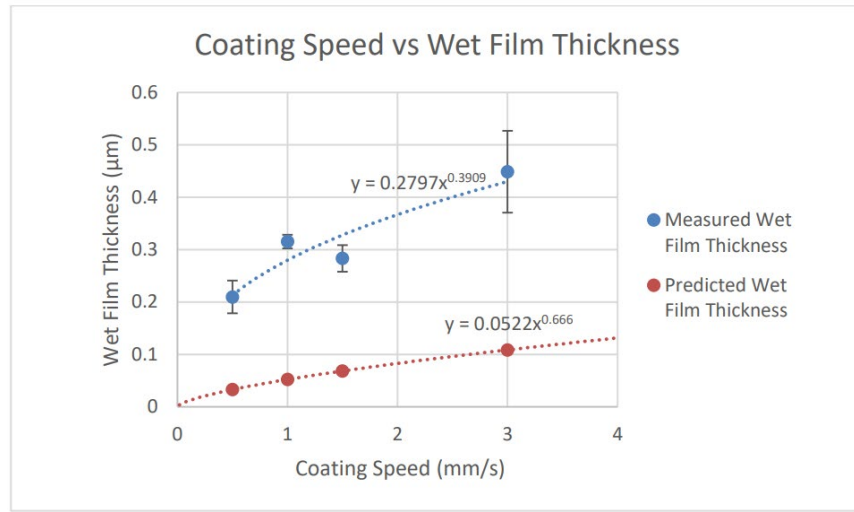

Figure 6: Plot showing predicted and measured wet film thicknesses achieved by the meniscus geometry of the blade coating device.

In our experiments, we observed that although the coating thickness did increase with increasing velocity, the curve fit had a lower power law exponent of 0.391 instead of the expected 0.667 from Equation 2. Additionally, the magnitude of the thickness is also around 5 times higher than predicted as opposed to the 2 – 3 times seen in the literature for this meniscus geometry.

Multilayer Coating Performance

The fabrication of multilayer samples using the slot-die coating process presented difficulties, including inconsistent features, unmanageable part thicknesses, and insufficient adhesion of deposited material to the substrate and to previous layers. This coating method struggled with the deposition of thin ink layers, and when coupled with the laser's limited sintering depth, it resulted in the creation of easily discernible bands of sintered and unsintered nanoparticles, as illustrated in the figure below.
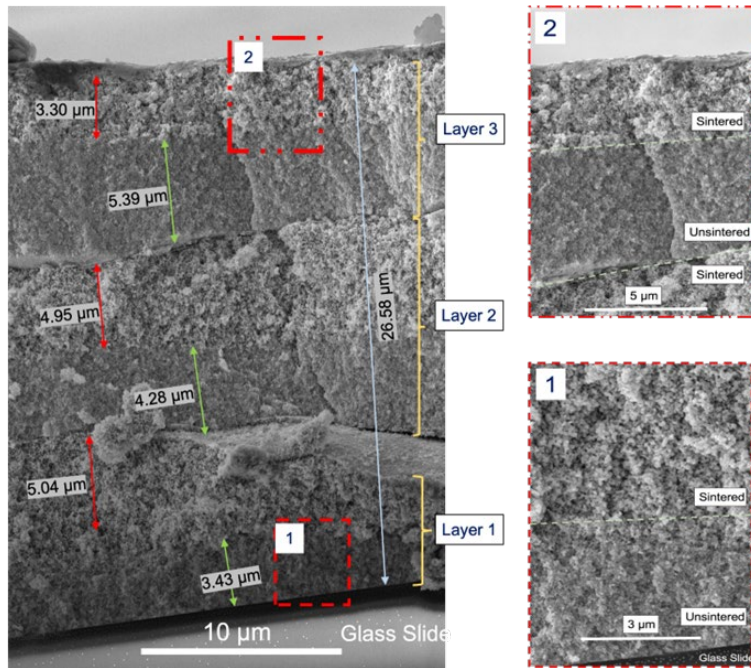
Figure 7: Cross section of multilayer coating process with the previous slot die coating process.

With the new coating process able to deposit submicron layers of ink (~ 0.3 μm), we can create structures that are fully sintered with no banding visible as shown in Figure 8 below. This leads to significantly improved interlayer adhesion which improves the final part strength and properties.
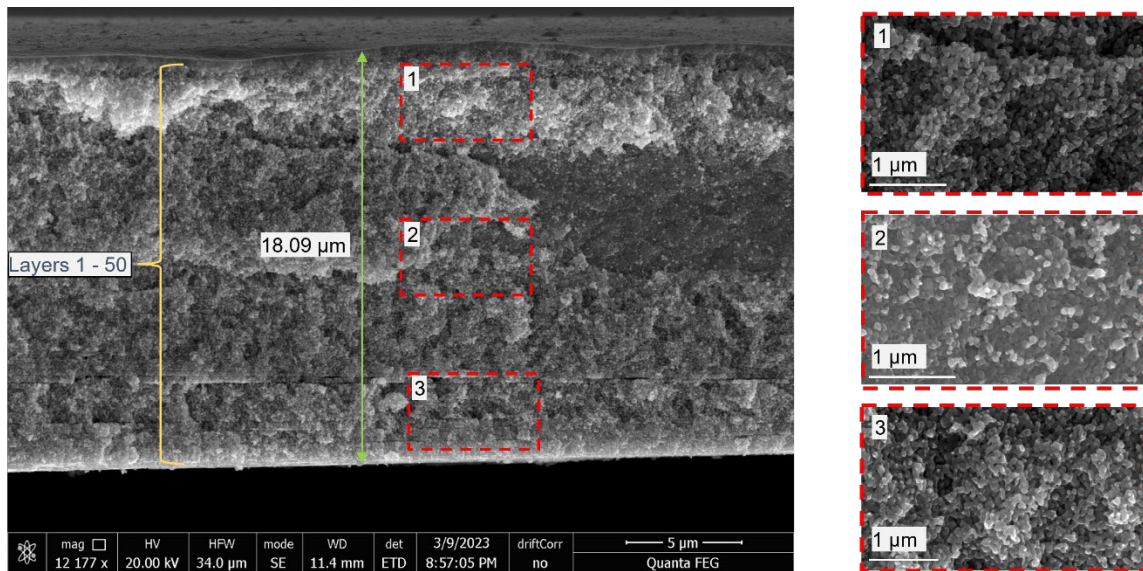

Figure 8: Cross section of the multilayer coating process using the newly designed blade coating process.

To test the stacking of multiple sintering regions, an 18-layer staircase structure was created using the laser masks below. Each of the images was projected by the DMD to heat up the particles in the white region of the mask, with each step using a smaller area to create a pyramid-like shape.
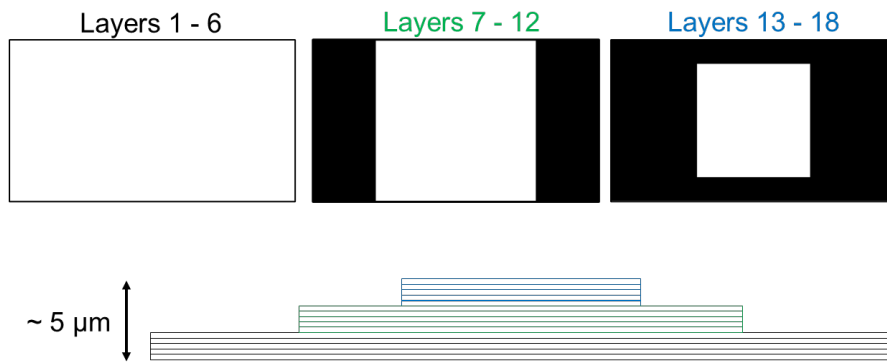
Figure 9: Three masks used to generate staircase pattern, and their respective layer numbers.
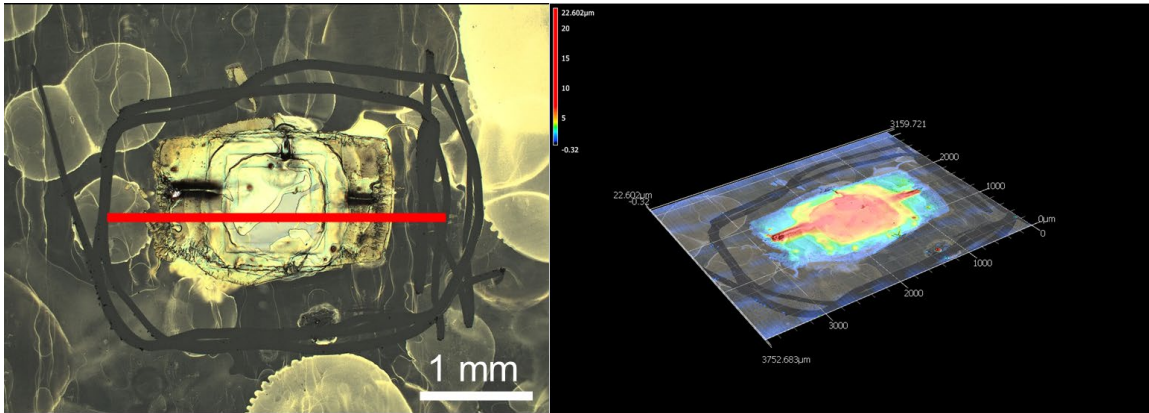

Figure 10: Staircase feature showing 3D capability of the µ-SLS process. Red line on left image shows where height profile was measured.

Each "staircase" step is comprised six consecutive layers of the same mask, which should roughly give a component with an approximate height of 5.8 µm. Considering that we anticipate roughly 0.3 µm per recoat in the coating process, the expected component height was projected to be around 5.4 µm. The envisioned profile was graphed and compared to the real profile along the center of the rectangle in the figure below.
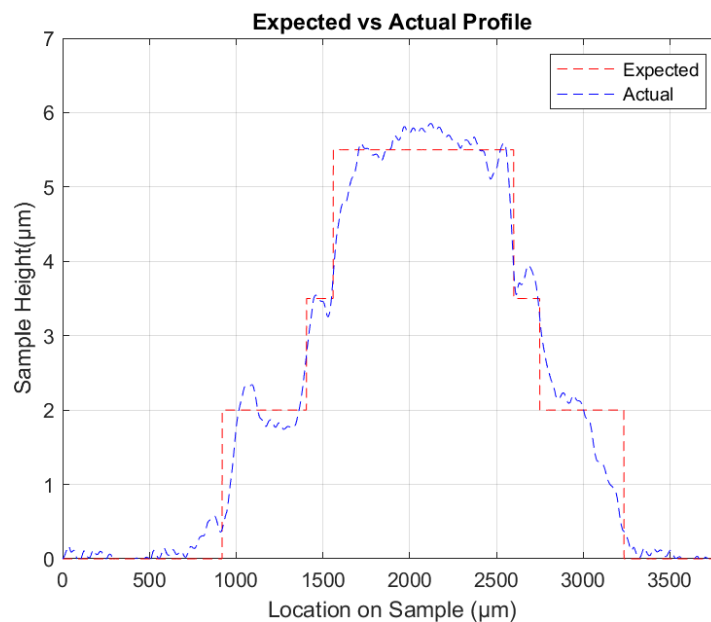

Figure 11: Averaged line profile across the center of the stacked pyramid structure.

The step heights closely align with the anticipated increment in layer height brought about by the blade coating process. In summary, we can see that this technique shows significantly improved vertical resolution compared to what was previously observed in the multilayer performance of the slot die coating process.

Conclusion

The objective of this work was to develop and evaluate a novel recoating process for the microscale selective laser sintering process to enable the creation of multi-layered structures. After an initial assessment of film deposition thickness, evaluation of improved sintering depth, and creating multilayer parts, it is evident that the blade recoating process has the capacity to deposit submicron layer thicknesses in a manner suitable for manufacturing multi-layered components. This process demonstrated reliable repeatability for components with fewer than 20 layers. However, achieving more precise control over layer thickness necessitates comprehensive characterization and a deeper exploration of the fundamental physics involved. This entails quantifying and comprehending the impact of coating operation parameters beyond just coating speed, including coating gap, ink volume, and blade angles. As the number of layers increases, a thorough understanding of these parameters becomes essential to maintain the recoating process's repeatability and prevent cumulative errors.

References

[1] N. K. Roy, D. Behera, O. G. Dibua, C. S. Foong, and M. A. Cullinan, "A novel microscale selective laser sintering (μ-SLS) process for the fabrication of microelectronic parts," *Microsyst Nanoeng*, vol. 5, no. 1, p. 64, Dec. 2019, doi: 10.1038/s41378-019-0116-8.

[2] N. K. Roy and M. Cullinan, "μ-SLS of Metals: Design of the powder spreader, powder bed actuators and optics for the system," presented at the Solid Freeform Fabrication, Austin, TX, Nov. 2015, pp. 134–155.

[3] N. K. Roy, C. S. Foong, and M. A. Cullinan, "Effect of size, morphology, and synthesis method on the thermal and sintering properties of copper nanoparticles for use in microscale additive manufacturing processes," *Additive Manufacturing*, vol. 21, pp. 17–29, May 2018, doi: 10.1016/j.addma.2018.02.008.

[4] M. Le Berre, Y. Chen, and D. Baigl, "From Convective Assembly to Landau−Levich Deposition of Multilayered Phospholipid Films of Controlled Thickness," *Langmuir*, vol. 25, no. 5, pp. 2554–2557, Mar. 2009, doi: 10.1021/la803646e.

[5] R. L. Davis, S. Jayaraman, P. M. Chaikin, and R. A. Register, "Creating Controlled Thickness Gradients in Polymer Thin Films via Flowcoating," *Langmuir*, vol. 30, no. 19, pp. 5637–5644, May 2014, doi: 10.1021/la501247x.